BIOCHEMISTRY
including biophysical chemistry & molecular biology
Article

Biochemistry **2009,** *48,* 5679–5688 5679
DOI: 10.1021/bi900242t

Effects of the N-Terminal Acylamido Group of Imidazole- and Pyrrole-Containing Polyamides on DNA Sequence Specificity and Binding Affinity[†]

Laura Westrate,[‡] Hilary Mackay,[‡] Toni Brown,[‡] Binh Nguyen,[§] Jerome Kluza,[∥] W. David Wilson,[§] Moses Lee,*[,‡] and John A. Hartley[∥]

[‡]*Division of Natural Sciences and Department of Chemistry, 35 East 12th Street, Hope College, Holland, Michigan 49422,* [§]*Department of Chemistry, Georgia State University, Atlanta, Georgia 30303, and* [∥]*Cancer Research UK Drug−DNA Interactions Research Group, UCL Cancer Institute, Paul O'Gorman Building, 72 Huntley Street, London WC1E 6BT, U.K.*

Received February 14, 2009; Revised Manuscript Received May 1, 2009

ABSTRACT: The N-terminal formamido group on imidazole- and pyrrole-containing polyamides causes stacked polyamides to bind in the minor groove of DNA in the staggered motif, and it also increases the binding affinity compared to those of non-formamido compounds. To further investigate the role of the N-terminal acylamido in affecting sequence specificity and binding affinity, six polyamide analogues containing the core triheterocyclic structure IPI were designed and synthesized, and the acylamido moiety reported herein includes the following: formamido (f-IPI, **1**), acetamido (Ac-IPI, **2**), trifluoroacetamido (Tf-IPI, **3**), *N*-methylureido (Mu-IPI, **4**), *N*-methylpyrrole-2-carboxamido (PIPI, **5**), and the ^{13}C-labeled formamido-IPI compound (^{13}C-f-IPI, **6**). In addition, two nonacylated IPI compounds were also synthesized and examined, namely, the amino-containing (NH_2-IPI, **7**) and non-formamido (nf-IPI, **8**) compounds. The binding characteristics of compounds **1**−**8** were investigated using methods of molecular biology and biochemistry, which included biophysical techniques, such as DNA melts, circular dichroism, isothermal titration calorimety, and surface plasmon resonance and DNase I footprinting. With the exception of nf-IPI and NH_2-IPI, all other compounds preferentially interacted with the cognate sequence, 5′-ACGCGT-3′. The biophysical results suggest that all six compounds bind within the minor groove at their cognate DNA sequence as stacked, staggered, antiparallel dimers. The order from highest to lowest binding affinities is as follows: f-IPI > P-IPI > Ac-IPI > Mu-IPI > Tf-IPI ≫ NH_2 and nf-IPI. Hence, having an acylamido moiety at the N-terminus is important for the binding of polyamides to DNA in a stacked and staggered motif. According to footprinting analysis, P-IPI (**5**), Ac-IPI (**2**), Mu-IPI (**4**), and Tf-IPI (**3**) exhibited some enhancement in sequence preference for their cognate 5′-ACGCGT-3′ over f-IPI (**1**). NMR analysis of the [^{13}C]f-IPI−CGCGnmr complex showed a slight downfield shift in the formamido ^{13}C signal indicating that the moiety remained intact. The trend in binding affinity suggests that steric factors play a role, in which small and planar aromatic acylamido units such as f, Ac, and P are preferred. Polar groups, such as in Mu-IPI (**4**) and Tf-IPI (**3**), afforded negative effects on binding affinity, compared to that of Ac-IPI (**2**).

Distamycin is a crescent-shaped, pyrrole-containing polyamide isolated from *Streptomyces*, found to successfully bind to the minor groove of DNA (*1*, *2*). It has been found to target A/T-rich sequences of DNA and preferentially binds as a stacked antiparallel dimer with the 5′-AAATTT-3′ sequence in a 2:1 fashion (*3*). It was discovered that stacked imidazole (I) and pyrrole (P) polyamides were capable of recognizing specific base pairs; a stacked P/P pairing recognizes either an A/T or T/A base pair, but a stacked I/P pairing recognizes a G/C base pair specifically (*4*−*7*). Subsequent studies, by the authors' laboratory, further revealed that the nature of the two core heterocycles had a dramatic effect on the binding affinity of the polyamide, with the following trend: IP > PP ≫ PI ≈ II (*8*). Most notably, the molecule f-IPI (**1**) bound to its cognate sequence (5′-ACGCGT-3′) with a binding affinity exceeding that of the other compounds studied, including the binding of distamycin to 5′-AAATTT-3′ (K_{eq} = 1.9 × 10^8 M^{-1} vs 1.7 × 10^7 M^{-1}, respectively). This trend concurs with a previous observation made by Dervan and co-workers with hairpin polyamides, in which they noted that a central IP pairing binds to DNA with a greater binding affinity than other hairpins studied with different heterocyclic cores (*9*).

Crucial to the binding of **1** is the N-terminal formamido group, which is also present in the natural product distamycin. This moiety has been found to favor stacking in a staggered fashion when two antiparallel monomers bind within the minor groove of DNA (*10*). The formamido group also has a dramatic effect in enhancing the binding affinity of the polyamide, up to 1000-fold

[†]We thank the NSF (Grants CHE 0550992 and 0809162) and Cancer Research UK (Grant C2259/A3083) for support.
*To whom correspondence should be addressed. Telephone: (616) 395 7190. E-mail: lee@hope.edu.

 Published on Web 05/06/2009

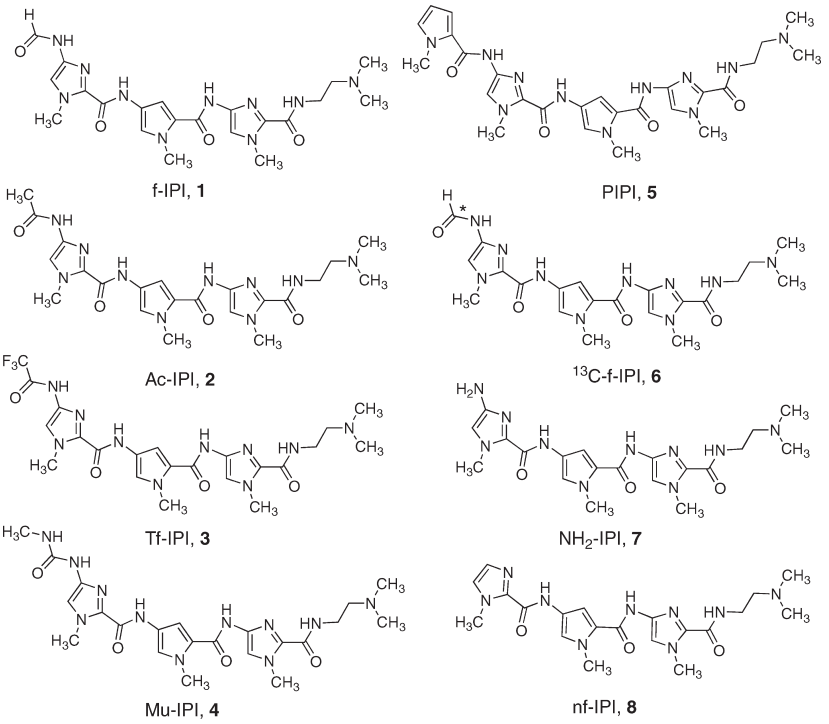

FIGURE 1: Structures of N-terminally modified IPI polyamides (**1**−**8**) used in this study.

higher when comparing formyl triamides with their non-formamido counterparts (*10*). However, although these effects on DNA binding have been well established, the underlying molecular nature of such effects is unclear. Thus, to further probe the nature of such effects, this report describes a systematic study performed with various N-termini (X) on the polyamide framework X-IPI (Figure 1).

In selecting the various N-terminal acylamido moieties, we considered several factors: steric requirements, polarity effects, and hydration. Considering sterics, the formamido group is relatively small and planar; thus, moieties with more or less bulk and nonplanar configurations were investigated, as well as removal of the acylamido group altogether. Dipole moments of polyamides have been demonstrated to affect how polyamides interact with DNA (*11*). Thus, groups with different polarities through the incorporation of halides and nitrogen atoms in the acylamido moiety were included in this study. Accordingly, the following molecules were chosen for this study: formamido (f-IPI, **1**), acetamido (Ac-IPI, **2**), trifluoroacetamido (Tf-IPI, **3**), *N*-methylureido (Mu-IPI, **4**), *N*-methylpyrrole-2-carboxamido (PIPI, **5**), and the ^{13}C-labeled formamido-IPI compound (^{13}C-f-IPI, **6**). This compound was designed to probe the possibility of hydration of the formamido group upon binding of **6** (or f-IPI, **1**) to DNA. Hydration of formamides and acetamides has been reported previously (*12*). In addition, two nonacylated IPI compounds were also studied, namely, the amino-containing NH_2-IPI (**7**) and non-formamido nf-IPI (**8**).

The synthesis of polyamides **1**−**8** is reported here together with their characteristics of binding to the cognate sequence (5′-ACGCGT-3′) when the molecules bind in a stacked−staggered motif. The T/G mismatch-containing sequence (5′-T/G-A-G/T-3′) contains the cognate site for the stacked−overlapped binding motif. Two other noncognate sequences (5′-ACCGGT-3′ and 5′-AAATTT-3′) are also included in the study (Figure 2). Binding characteristics were determined by thermal denaturation (ΔT_m), circular dichorism (CD), isothermal titration microcalorimetry (ITC), surface plasmon resonance (SPR), and DNase I footrpinting.

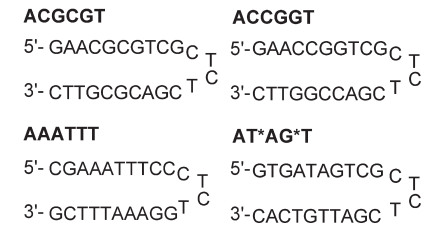

FIGURE 2: DNA sequences used to study the binding affinity and selectivity of the polyamides ACGCGT, ACCGGT, AAATTT, and AT*AG*T.

MATERIALS AND METHODS

Synthesis. Polyamides **1**, **5**, and **8** were synthesized according to previously published methods (*13*, *14*). Solvents and organic reagents were purchased from Aldrich or Fisher and were used without further purification with the exception of DCM (P_2O_5) and DMF (BaO) which were distilled prior to use. Melting points (mp) were performed using a Mel-temp instrument and are uncorrected. Infrared (IR) spectra were recorded using a Midac M1700 FT-IR instrument as films on NaCl disks. NMR spectra were recorded on a Varian INOVA 400 MHz instrument. Chemical shifts (δ) are reported at 20 °C in parts per million downfield from internal tetramethylsilane. High-resolution mass spectra (HRMS) and low-resolution mass spectra (LRMS) were provided by the Mass Spectrometry Laboratory of the University of South Carolina (Columbia, SC). Reaction progress was assessed by thin-layer chromatography (TLC) using Merck silica gel (60 F_{254}) on aluminum plates. Visualization was achieved with UV light at 254 and/or 366 nm, I_2 vapor staining, and ninhydrin spray.

*(i) Ac-IPI (**2**)*. NO_2-IPI (**9**) (50 mg, 0.11 mmol) was reduced to amine **7** in the presence of hydrogen over 5% Pd/C (50 mg,

100% by weight) using a previously published method (*15*). Acetic anhydride (0.1 mL, 0.98 mmol) was then added dropwise to a chilled (ice−water bath) stirring solution of the amine containing DIPEA (80 mg, 0.62 mmol), DMAP (1.5 mg, 0.012 mmol), and dry DCM (5 mL). The reaction mixture was allowed to warm to room temperature (RT) overnight and then rechilled in an ice−water bath, and the reaction was quenched with a dropwise addition of MeOH (2 mL). The mixture was evaporated to dryness and redissolved in $CHCl_3$ (75 mL) and water (15 mL). The aqueous layer was basified to a pH of ~12 with 1 M NaOH, and the $CHCl_3$ layer was collected. The aqueous layer was re-extracted with $CHCl_3$ (50 mL) and EtOAc (2 × 50 mL). The combined organic extracts were dried over anhydrous Na_2SO_4 and reduced in vacuo. The residue was then purified via flash column chromatography [silica gel, gradient from 0% $CHCl_3$ and 100% MeOH to 100% $CHCl_3$ and 0% MeOH (v/v)] to yield compound **2** as a brown solid (19.7 mg, 36%): mp 129−134 °C; R_f = 0.18 [80:20 (v/v) $CHCl_3$/MeOH]; ^{1}H NMR (400 MHz, $CDCl_3$) δ 9.33 (br s, 1H), 9.28 (br s, 1H), 8.40 (br s, 1H), 7.39 (s, 1H), 7.36 (d, J = 1.6 Hz, 1H), 7.35 (s, 1H), 6.81 (d, J = 1.6 H_3, 1H), 4.02 (s, 3H), 3.98 (s, 3H), 3.93 (s, 3H), 3.53 (t, J = 6.0 Hz, 2H), 2.71 (t, J = 6.0 Hz, 2H), 2.43 (s, 3H); IR (neat) 3300, 2943, 2857, 1652, 1556, 1385, 1148, 1090 cm^{-1}; MS (ES$^+$) m/z (relative intensity) 499 ([M + H], 70%), 250 (20%); HRMS for $C_{22}H_{31}N_{10}O_4$ calcd 499.2529, observed 499.2518.

*(ii) Tf-IPI (**3**).* NO_2-IPI (103 mg, 0.21 mol) was reduced with 5% Pd/C (52 mg, 50% by weight) to yield amine **7** which was then dissolved in dry DCM (3 mL). TFA (1 mL) was added to acetic anhydride (2 mL) and the mixture stirred over ice before being heated to 50 °C for 50 min and then recooled to 0 °C. This acetic trifluoroacetic anhydride solution was then added dropwise to the amine solution at 0 °C and allowed to stir for ~18 h (from 0 °C to RT). The reaction was then quenched with the addition MeOH (30 mL), with stirring at 0 °C for ~1 h. After basic-aqueous extraction, as described for **2**, the residue was purified over silica gel [gradient from 0% $CHCl_3$ and 100% MeOH to 100% $CHCl_3$ and 0% MeOH (v/v)] to yield compound **3** as a cream crystalline solid (36 mg, 31%): mp 167 °C; R_f = 0.14 (80:20 $CHCl_3$/MeOH); ^{1}H NMR (400 MHz, $CDCl_3$) δ 7.47 (s, 1H), 7.42 (d, J = 2.0 Hz, 1H), 7.42 (s, 1H), 6.83 (d, J = 2.0 Hz, 1H), 4.08 (s, 3H), 4.00 (s, 3H), 3.96 (s, 3H), 3.55 (t, J = 6 Hz, 2H), 2.45 (br s, 2H); IR (neat) 3272, 3152, 3014, 2947, 2916, 1669, 1538, 1442, 1407, 1207, 1185, 1127, 1064, 1021 cm^{-1}; MS (ES$^+$) 553 ([M + H], 100%); HRMS for $C_{22}H_{28}F_3N_{10}O_4$ calcd 533.2247, observed 553.2244.

*(iii) Mu-IPI (**4**).* NO_2-IPI (**9**) (62 mg, 0.13 mmol) was reduced as described above, and the resulting amine **7** was dissolved in DCM (5 mL). Methyl isocyanate (500 mg) was dissolved in dry DCM (2 mL) and added to the reaction mixture at 0 °C, and then the mixture was allowed to stir at RT for 19 h. The crude product was purified as described above to yield compound **4** as a brown solid (65.9 mg, 21%): mp 83−85 °C; R_f = 0.14 [70:30 (v/v) $CHCl_3$/MeOH]; ^{1}H NMR (400 MHz, CD_3OD) δ 7.83 (s, 1H), 7.41 (s, 1H), 7.41 (s, 1H), 7.32 (d, J = 1.6 Hz, 1H), 7.04 (d, J = 2.0 Hz, 1H), 6.95 (s, 1H), 4.02 (s, 3H), 4.02 (s, 3H), 3.94 (s, 3H), 3.62 (t, J = 5.6 Hz, 2H), 2.99 (t, J = 5.6 Hz, 2H), 2.83 (s, 6H); IR (neat) 3300, 2924, 2852, 1658, 1538, 1469, 1405, 1249, 1207, 1121, 1061, 1019, 753 cm^{-1}; MS (ES$^+$) m/z (relative intensity) 514 ([M + H], 60%), 273 (100%), 258 (40%); HRMS for $C_{22}H_{32}N_{11}O_4$ calcd 514.2638, observed 514.2657.

*(iv) ^{13}C-f-IPI (**6**).* The synthesis of this compound was conducted as described for **1** (*14*), except a 99% ^{13}C-labeled formic acid was used to generate the acetic formic anhydride. The target compound **6** was isolated as a tan crystalline solid (81 mg, 78%): mp 100 °C; R_f = 0.30 [90:10 (v/v) $CHCl_3$/MeOH]; ^{1}H NMR (400 MHz, $CDCl_3$) δ 8.86 (br s, 1H), 8.63 (br s, 1H), 8.30 (br s, 1H), 8.13 (br s, 1H), 7.72 (br t, 1H), 7.45 (s, 1H), 7.42 (s, 1H), 7.29 (d, 1H, J = 2.0 Hz), 6.80 (d, 1H, J = 2.0 Hz), 4.07 (s, 3H), 4.02 (s, 3H), 3.96 (s, 3H), 3.54 (q, J = 6.0 Hz, 2H), 2.55 (t, J = 6.0 Hz, 2H), 2.31 (s, 6H); ^{13}C NMR ($CDCl_3$) δ 157.71 (s); IR (neat) 3282, 3173, 2951, 2860, 2824, 2779, 1657, 1534, 1469, 1443, 1405, 1250, 1121, 754 cm^{-1}; MS (ES$^+$) m/z (relative intensity) 486 ([M + H], 100%).

*(v) NH_2-IPI (**7**).* Compound **9** (127 mg, 0.28 mmol) was reduced as described above and dried over P_2O_5 in vacuo to yield **7** as a yellow solid (protected from light) (95 mg, 75%): mp 114 °C dec; R_f = 0.07 [80:20 (v/v) $CHCl_3$/MeOH]; ^{1}H NMR (400 MHz, $CDCl_3$) δ 8.87 (br s, 1H), 8.08 (br s, 1H), 7.57 (br s, 1H), 7.41 (s, 1H), 7.25 (s, 1H), 6.78 (s, 1H), 6.34 (s, 1H), 4.04 (s, 3H), 4.01 (s, 3H), 3.97 (s, 3H), 3.48 (q, J = 5.2 Hz, 2H), 2.53 (t, J = 5.2 Hz, 2H), 2.32 (s, 6H); IR (neat) 3337, 2953, 2827, 1655, 1537, 1468, 1446, 1406, 1366, 1256, 1206, 1122, 1056, 1022 cm^{-1}; MS (ES$^+$) m/z (relative intensity) 457 ([M + H], 100%), 448 (50%), 229 (70%), 115 (35%); HRMS for $C_{20}H_{29}N_{10}O_3$ calcd 457.2424, observed 457.2424.

Thermal Denaturation. The synthetic DNA hairpins used in these studies were obtained from Operon (Huntsville, AL) with no HPLC purification: ACGCGT, 5′-GAACGCGTCGCTCT-CGACGCGTTC; ACCGGT, 5′-GAACCGGTCGCTCTCGA-CCGGTTC; AAATTT, 5′-CGAAATTTCCCTCTGGAAAT-TTCG; and AT*AG*T, 5′-GTGATAGTCGCTCTCGATTG-TCAC. Thermal denaturation data were obtained using a Cary Bio 100 spectrophotometer and cells with a 10 mm path length using a previously reported method (*16*). Duplicate experimental data were analyzed using KaleidaGraph (Synergy Software, Reading, PA) and the melting temperature (T_m) values determined as the maximum of the first derivative.

Circular Dichroism (CD). CD studies were performed on an OLIS (Bogart, GA) DSM20 spectropolarimeter using a 1 mm path length cuvette and a band-pass of 2.4 nm as described previously (*17*) with the exception of the integration time, which was set to integrate as a function of PMT high volts. Experiments were conducted in duplicate and the data analyzed using KaleidaGraph.

Isothermal Titration Calorimetry (ITC). ITC analysis was performed at 25 °C using a VP-ITC micromalorimeter (MicroCal, Northampton, MA) as previously reported (*13*). Origin 7.0 was used to analyze the data, where the integration of each titration was plotted against ligand concentration. A linear fit was then employed, and this was subtracted from the reaction integrations to normalize for nonspecific heat components. A two-site, nonsequential model was then fitted to the curve and used to determine the binding constant, K_{eq} (*10*, *18*).

Surface Plasmon Resonance (SPR). Biosensor chip surface preparations and biotinylated DNA immobilizations were conducted as previously described (*19*) with the following biotin-labeled DNA hairpins: 5′-biotin-GA**ACGCGT**CCTCTGACG-CGTTC, 5′-biotin-GA**ACCGGT**CCTCTGACCGGTTC, and 5′-biotin-CG**AAATTT**CCTCTGAAATTTCG (purchased from Midland Certified Reagent Co. with HPLC purification). Experiments were conducted in a phosphate buffer at 200 mM Na^+ and 0.0005% P20 surfactant on a BIACORE 2000 instrument. Ligand (250 μL) was injected with a flow rate of 50 μL/min (f-IPI, Ac-IPI, and Mu-IPI) or 20 μL/min (Tf-IPI) followed with

a 15 min period for dissociation. The sensor chip surface was regenerated with a glycine pH 2.5 solution or a 0.5 min injection of a 0.4 M NaCl/20 mM NaOH solution followed by multiple buffer injections. Kinetic analyses were performed for sensorgrams that did not reach the steady state as previously described (*10*), and the averaged binding constants were calculated from the rate constants. For sensorgrams that reach the steady state, steady-state analyses were conducted and the response units were converted to moles of ligand per mole of hairpin as previously described (*8*, *10*). The data were fitted with eq 1 to obtain macroscopic binding constants.

$$r = (K_1 C_{free} + 2K_1K_2C_{free}^2)/(1 + K_1C_{free} + K_1K_2C_{free}^2) \quad (1)$$

Nuclear Magnetic Resonance (NMR). A self-complementary DNA decamer was purchased from Operon with no HPLC purification with the sequence 5′-CCACGCGTGG (termed CGCGnmr). The lyophilized oligonucleotide was suspended in a 10 mM sodium phosphate buffer (pH 7.2) prepared with 99.96% D_2O to give a 0.5 mM solution of double-stranded DNA. An aliquot of this stock solution was transferred to an NMR tube such that the tube contained ~30 μmol of DNA (determined more accurately by UV−vis to be 28.6 μmol). A polyamide solution (protonated with 1 molar equiv of HCl, 5 mM in 10 mM phosphate D_2O buffer) was added to the NMR tube to yield a 2:1 DNA:polyamide ratio. The sample was lyophilized and redissolved in 99.96% D_2O twice to remove any H_2O and dried thoroughly under vacuum overnight. This was then resuspended in 100% D_2O, and ^1H NMR spectra were acquired and compared to those previously reported for f-IPI (**1**) (*14*). A ^{13}C spectrum was then acquired using the following settings: number of full induction decays, 30000; sweep width, 25000 Hz; line broadening, 2; and *T*, 25 °C. An external $CDCl_3$ standard was set to 77 ppm.

DNase I Footprinting: Preparation of the DNA Substrate, Radiolabeling, and Purification and DNase I Footprinting Experiments. Two 130 bp fragments were amplified by using PCR as follows. The forward primer 5′-GTCGTTAGGAGAGCTCACTTG-3′ (4 ng) was radioactively labeled by treatment with γ-^{32}P (3 μL) and 1 μL of T4 polynucleotide kinase (Invitrogen) following the standard protocols. PCR was performed in thermophilic DNA polybuffer containing dNTPs (50 μL, 125 μM), $MgCl_2$ (1 mM), Flexi Taq polymerase (1 unit), and ^{32}P-labeled forward primer, reverse primer 5′-CTCCAGAAAGCCGGCAACTCAG-3′ and IM18 5′-ATGCTCCA GAAAGCCGGCACTCAGTCTACAAACGCGTCATCTTGATCATGCATGTTCACAGAAATTTCTCTAGATCTTAGCTTAACTCTAGTACTAGTCTTCAAGCAAGTGGAGCTCTCCTAACCGACTTT-3′ (20 ng) and IM20 5′-AAAGTCGGTTAGGAGAGCT CCACTTGCTTGAAGACTAGT ACTAGAGTTAAGCTAAGATCTAGAGAAATTTCTGTGAACATGCATGATCAAGATGACGCGTTTGTAGACTGAGTGCCGGCTTT CTGGAGCAT-3′ (20 ng), or both templates, IM23 5′-ATGCTCCAGAAAGCCGGCACTCAGTCTACAAACGCGTCATCTTGATCACCGGTGTTCACAGAAATTTCTCTAGATCTACGTGTAACTCTAGTAGCGCTCTTCAAGCAAGTGGAGCTCTCCTAACCGACTTT-3′ (20 ng) and IM24 5′-AAGTCGGTTAGGAGAGCTCCACTTGCTTGAAGAGCGCTACTAGAGTTACACGTAGATCTAGAGAAATTTCTGTGAACACCGGTGATCAAGATGACGCGTTTGTAGACTGAGTGCCGGCTTTCT GGAGCAT-3′ (20 ng).

Polymerase chain reaction was conducted as follows: an initial denaturation step for 3 min at 95 °C and 1 min at 94 °C, 1 min at 63 °C, and 1 min at 72 °C for 35 cycles. The PCR products were purified by 2% agarose gel electrophoresis. Finally, DNA was isolated by using the Mermaid Kit (Q-biogene) according the manufacturer's instructions.

Footprinting experiments were performed essentially as described previously (*20*). Briefly, reactions were conducted in a total volume of 8 μL. For each sample, 200 cpm of radiolabeled DNA was used. Samples (2 μL) of the labeled DNA fragment were incubated with 4 μL of the buffered solution [10 mM Tris base and 10 mM NaCl (pH 7)] containing the drug at the appropriate concentration. After incubation for 30 min at room temperature to ensure equilibration of the binding reaction mixture, the digestion was initiated by the addition of 2 μL of a DNase I solution [20 mM NaCl, 2 mM $MgCl_2$, and 2 mM $MnCl_2$ (pH 8)] whose concentration was adjusted to yield a final enzyme concentration of 0.01 unit/mL in the reaction mixture. The reaction was stopped by freeze-drying the mixture after 3 min. Samples were lyophilized and dissolved in 4 μL of an 80% formamide solution containing tracking dyes. The DNA samples were then heated at 95 °C for 3 min and chilled in ice for 3 min before electrophoresis. Electrophoresis was performed for 2.5 h (70 W, 50 °C) in TBE buffer [89 mM Tris base, 89 mM boric acid, and 2.5 mM Na_2EDTA (pH 8.3)]. The gel was transferred onto Whatman 3MM paper and dried under vacuum at 80 °C for 2 h. The gel was exposed overnight to X-ray film (Super RX, Fuji).

RESULTS AND DISCUSSION

Synthesis. Polyamides f-IPI (**1**) (*14*), PIPI (**5**), and nf-IPI (**8**) (*13*) were synthesized following previously reported methods. The synthetic strategy for preparing the other compounds described in this paper is given in Scheme 1. Catalytic hydrogenation of the nitro group of NO_2-IPI (**9**) over palladium on carbon afforded the amino product NH_2-IPI (**7**). In separate reactions, in situ coupling of amine **7** with acetic anhydride, trifluoroaccetic anhydride, acetic [^{13}C]formic anhydride, and methyl isocyanate provided the acetamido-IPI (**2**), trifluoroacetamido-IPI (**3**), ^{13}C-labeled f-IPI (**6**), and methylureido-IPI (**4**), respectively, in reasonable yields. All compounds gave excellent purity according to ^1H NMR analysis, and the structures were confirmed through NMR, IR, and mass spectral analyses.

Thermal Denaturation Experiments. Thermal denaturation experiments were performed using four different DNA sequences (Figure 2) to determine if the compounds with alternative N-termini were capable of stabilizing the DNA at elevated temperatures. The DNA sequences included the cognate sequence for staggered binding of the IPI core ACGCGT, and the cognate for overlapped binding of the IPI core AT*AG*T, where T* and G* indicate T·G and G·T mismatch base pairs, respectively. Two noncognate sequences were included as negative controls: the A/T-rich sequence AAATTT and a C/G-rich sequence ACCGGT. The results listed in Table 1 reveal that only compounds PIPI (**5**) and Ac-IPI (**2**) bound to the staggered cognate sequence with sufficient affinity to cause stabilization of the DNA at elevated temperatures (ΔT_m = 3 and 2 °C, respectively). Additionally, both **2** and **5** demonstrated selectivity for the staggered cognate with this technique as ΔT_m values of 0 °C were obtained with the other DNA sequences. In comparison, thermal denaturation studies have shown that f-IPI (**1**) binds with a higher level of affinity to the staggered cognate sequence,

Table 1: ΔT_m Values, Concentrations of Ligand at Which Footprint Appears, SPR-Derived Binding Constants, and ΔH Values Obtained from ITC for Compounds **1**−**5**, **7**, and **8** with ACGCGT

compound	ΔT_m (°C)	footprint (μM)[e]	K_{eq} (M^{-1})[f]	ΔG[g] (kcal/mol)	ΔH[h] (kcal/mol)	$T\Delta S$[i] (kcal/mol)
f-IPI (**1**)[a]	9	0.05	1.9×10^8	−11.3	−7.6	3.7
Ac-IPI (**2**)	2	0.1	2.1×10^6	−8.6	−5.2	3.4
Tf-IPI (**3**)	0	5	2.6×10^5	−7.4	−3.1	4.3
Mu-IPI (**4**)	0	1	5.0×10^5	−7.8	no heat	−
PIPI (**5**)[b]	3	0.5	7.1×10^6	−9.3	−3.2	6.1
H_2N-IPI (**7**)	0	10−20	nd[c]	−	nd[d]	−
nf-IPI (**8**)	0	none	nd[d]	−	nd[d]	−

[a] From ref (*14*). [b] From ref (*13*). [c] Not determined because polyamide **7** adhered to the plastic tubing of the Biacore SPR instrument. [d] Not determined because it did not show any indication of binding by all other methods. [e] Lowest dose at which footprinting at the cognate 5′-ACGCGT-3′ sequence was observed. [f] $K_{eq} = (K_1K_2)^{1/2}$. [g] $\Delta G = -RT \ln K_{eq}$. [h] $\Delta H = (\Delta H_1 + \Delta H_2)/2$ (experiment run in duplicate). [i] Calculated from $\Delta G = \Delta H - T\Delta S$.

Scheme 1: Synthetic Scheme for the Synthesis of Compounds **2**−**4**, **6**, and **7**[a]

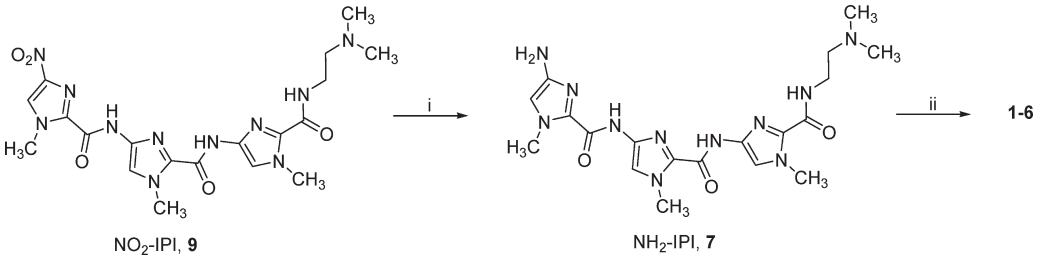

[a] (i) 5% Pd/C, cold MeOH, H_2, RT, 18 h; (ii) for Ac-IPI (**2**), acetic anhydride, Hunig's base, DMAP, dry DCM, from 0 °C to RT, 18 h; for Tf-IPI (**3**), acetic trifluoroacetic anhydride, dry DCM, from 0 °C to RT, 18 h; for Mu-IPI (**4**), methyl isocyanate, dry DCM, from 0 °C to RT, 18 h; for ^{13}C-f-IPI (**6**), acetic [^{13}C]formic anhydride, dry DCM, from 0 °C to RT, 18 h. Syntheses of **1** (*14*), **5**, and **8** (*13*) have been reported.

(ΔT_m = 9 °C); however, the ΔT_m values for **1** binding to ACCGGT and AAATTT were found to be 1 °C in both cases. ^{13}C-f-IPI (**6**) behaved identically to f-IPI (**1**) as anticipated. Non-formyl-IPI (**8**), which should bind in an overlapped fashion, did not stabilize the AT*AG*T sequence or any of the other sequences. Neither did amino-IPI (**7**), Tf-IPI (**3**), or MU-IPI (**4**).

Circular Dichroism (CD). CD experiments were conducted with the five novel compounds (**2**−**4**, **6**, and **7**) and the four DNA sequences outlined above, and the results were compared to results obtained previously for **1**, **5**, and **8**. The polyamide solution was titrated into the DNA in 1 molar equiv increments until past the point of saturation of the induced peak at ~320 nm, which is indicative of binding of the ligands in the minor groove (*21*). Moreover, the properly defined isodichroic points on the titration spectra further suggest that the ligands bind to the DNA through a single mechanism, presumably minor groove binding. Figure 3 shows the CD plots of Ac-IPI (**2**), Tf-IPI (**3**), Mu-IPI (**4**), H_2N-IPI (**7**), and f-IPI (**1**). Plots of PIPI (**5**) have been previously published (*13*); ^{13}C-f-IPI (**6**) gave results identical to those of **1**, and nf-IPI (**8**) showed very little or no binding to any of the sequences, including the T/G mismatched sequence (AT*AG*T). Thus, spectra for these compounds are not shown in this report. It can be observed that titration of Ac-IPI (**2**) to the cognate sequence ACGCGT gave the highest DNA-induced ligand band at ~320 nm (saturation observed at a molar ratio of 2:1 for ligand to DNA) which is comparable to the parent molecule **1**. It is closely followed by Tf-IPI (**3**), which showed a saturation of the DNA-induced band at a 3:1 ligand:DNA molar ratio. Although Mu-IPI (**4**) and H_2N-IPI (**7**) yielded a similar CD response to **2** and **3**, they did not show saturation with the cognate sequence. This implies that they may not bind as strongly to this DNA as polyamides **1**−3 and PIPI (**5**) (*8*, *20*). Moderately strong induced bands were also observed for **2**−4 with the noncognate sequence ACCGGT, which was also the case with f-IPI (**1**). Less moderate bands were also recorded for AAATTT, however, to a lesser degree than the parent molecule, potentially corroborating the increased selectivity of these compounds also seen in the thermal denaturation experiments. None of the compounds tested bound to the T/G mismatch-containing sequence (AT*AG*T) with any significance, suggesting that the alternate *N*-acylamido moieties do not compromise the ability of the monomers to bind in the staggered motif. Removal of an acylamido group significantly compromised binding affinity.

Biosensor Surface Plasmon Resonance (SPR). SPR analysis was carried out on compounds **2**−**4** and **7** to determine their binding affinity (K_{eq}) with three DNA sequences (ACGCGT, ACCGGT, and AAATTT), and selected results are given in Figure 4 along with the previously published f-IPI (**1**) sensorgrams for comparison (*14*). It is immediately apparent from these results that compounds **2**−**4** bind preferentially to their cognate sequence (ACGCGT) over the noncognate sequence (ACCGGT). It can also be observed that these compounds demonstrate a higher degree of selectivity than the parent f-IPI (**1**) which shows some binding to ACCGGT. Also of interest are the binding kinetics. Notably, the dissociation rate of f-IPI (**1**) is quite slow; rates for Ac-IPI (**2**), Mu-IPI (**4**), and PIPI (**5**) (*13*) are intermediate, while the rate for Tf-IPI (**3**) is quite fast. Unfortunately, SPR analysis could not be carried out on NH_2-IPI (**7**) as this polyamide had a propensity to stick to the plastic tubing and other surfaces of the instrument. Since nf-IPI (**8**) did not show significant DNA binding affinity by the other methods (including DNase I footprinting which will be described later), it was not tested by SPR.

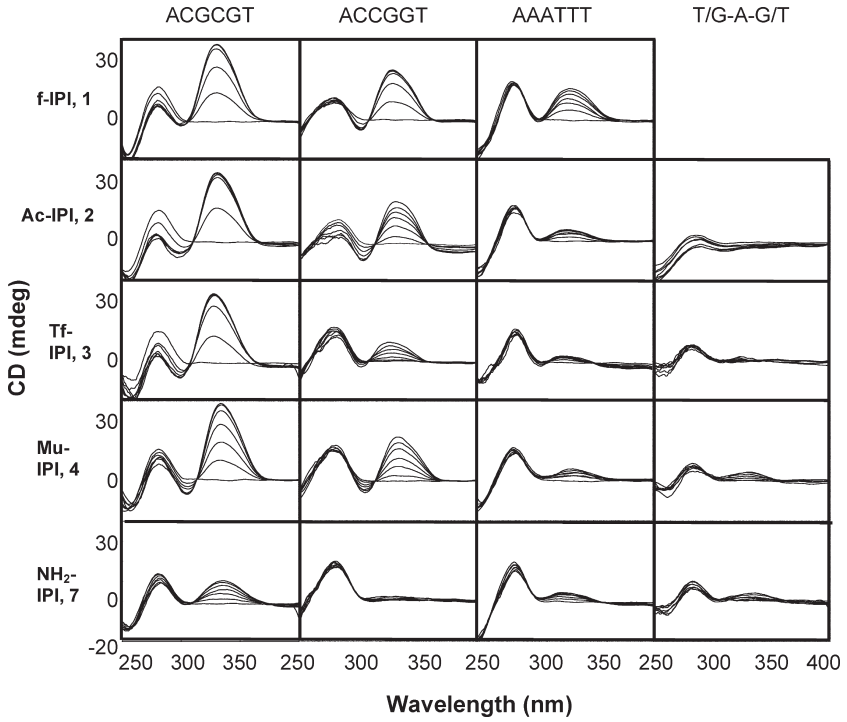

FIGURE 3: CD spectra of compounds **1**, **3**−**5**, and **7** binding to the four DNA sequences. Polyamides were titrated to a 9 μM DNA solution in aliquots of 1 molar equiv (through 6 molar equiv) in 10 mM phosphate buffer [1 mM EDTA and 50 mM Na^+ (pH 6.2)]. Data were obtained using an OLIS DSM20 spectropolarimeter.

Fitting the normalized responses versus ligand concentration and using a two-site model (Figure 5B), we ascertained the binding constants for compounds **2**−**4**, and they are listed in Table 1. It can be observed that none of the compounds synthesized with the alternative N-terminal acylamido groups display a higher binding constant than f-IPI (**1**). However, it should be noted that compounds **2**−**5** exhibited a higher level of selectivity for ACGCGT than the formamido parent molecule f-IPI. According to the binding constants, the order of descending strength is as follows: f-IPI (**1**) > PIPI (**5**) > Ac-IPI (**2**) > Mu-IPI (**4**) > Tf-IPI (**3**). Interestingly, compared to the acetyl moiety, addition of polar groups to the acylamido group (Tf and Mu) negatively impacted binding affinity. However, binding of the stacked polyamides to ACGCGT was found to be positively cooperative, in which the binding constant of the "second" molecule is greater than that of the "first" molecule (K_2 > K_1) (*8*, *13*, *14*). This is an interesting discovery because "Ac," "Mu", and "Tf" groups are bulkier than the formamido group yet are capable of binding to the minor groove as a staggered and stacked dimer. This is consistent with earlier reports showing that Ac-containing polyamides, including hairpin polyamides, are able to bind in the "stacked" configuration in the minor groove, albeit with reduced affinity compared to their formamido counterparts (*22*). The authors have suggested using results obtained from an NMR study on complexes of hairpin polyamides with DNA that N-terminal acetylation leads to an intramolecular steric clash for hairpin ligands bound in the minor groove, promoting rotation of the spatially close C-terminal heterocycle (*22*). This could explain the reduced affinity of the bulkier polyamides **2**−**4** versus f-IPI (**1**). To gain further insight into the steric hindrance−affinity relationship, we calculated the molar volumes of four acylamido groups found in polyamides **1**−**4** using Molinspiration (*23*). The values are 42.907, 59.468, 74.205, and 71.870 $Å^3$, respectively. The values provided a linear and inverse relationship (data not shown) between molar volumes and binding affinities (see Table 1) expressed in ln K_{eq}; as the molar volume increased, affinity decreased. The pyrrole-2-carboxamido-containing compound (PIPI, **5**) was not included in this analysis because it is structurally quite different from the simpler acylamido groups found in compounds **1**−**4**; hence, the results would not be directly comparable.

Finally, although SPR studies were not conducted on amino-IPI (**7**) and nf-IPI (**8**), on the basis of DNA melts, CD, and ITC studies, as well as DNase I footprinting studies, it can be extrapolated that their binding constants would be significantly lower than those noted above.

Isothermal Titration Microcalorimetry (ITC). The thermodynamic parameters that govern the interactions of polyamides with DNA can be evaluated using ITC. Experiments were conducted with the five novel compounds (**2**−**4**, **6**, and **7**) and the four DNA sequences outlined above, and the results were compared to results obtained previously for **1** and **5**. ITC analyses were not conducted for nf-IPI **8** as it did not show significant binding with the previous techniques. Of the novel compounds, only **2**, **3**, and **6** registered heat release, and only on binding to the staggered cognate sequence. Compound **6** yielded a thermogram comparable to that previously published for **1** (*14*) as anticipated and is thus not shown here, and the thermogram for PIPI (**5**) has been published previously (*13*). The thermograms for Ac-IPI (**2**) and Tf-IPI (**3**) are depicted in Figure 5, and the enthalpy values are listed in Table 1. It is noteworthy that alteration of the formamido group has a significant effect on the enthalpic component of the binding thermodynamics. As the *N*-acylamido group becomes bulkier, such as Tf and P (molar volume of 1-methylpyrrole-2-carboxamide is 116.244 $Å^3$), the entropic component of the binding predominates. The same trend was observed for Mu-IPI (**4**), in which Mu is bulkier than Tf and Ac. It has negligible enthalpy of binding; hence, the thermodynamics of binding as evidenced by SPR studies must come almost entirely from entropic gains. These results provide information

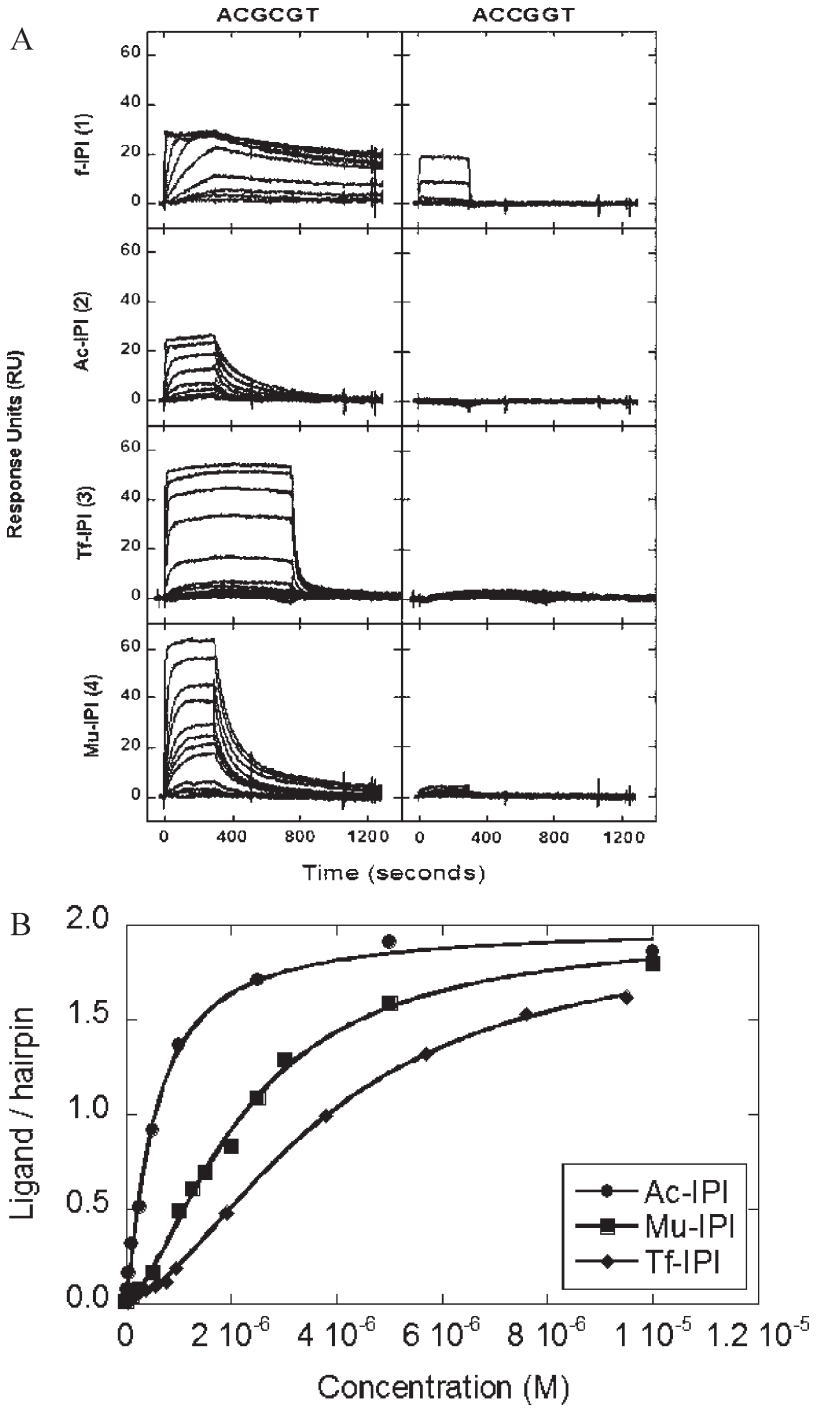

FIGURE 4: (A) SPR sensorgrams of f-IPI (**1**), Ac-IPI (**2**), Tf-IPI (**3**), and Mu-IPI (**4**) binding to ACGCGT (left) and to ACCGGT (right). (B) Binding isotherms for Ac-IPI, Tf-IPI, and Mu-IPI with the ACGCGT hairpin as seen in panel A.

that shows that the formamido group must interact with DNA through a mechanism that garners favorable enthalpy. Even though the mechanism of interaction is unclear, it was thought that there might be a possibility that the formamido group might become hydrated when bound to DNA.

NMR Studies. To gain further insight into what the *N*-formamido group of IPI might undergo upon binding to ACGCGT, a ^{13}C-labeled f-IPI (**6**) polyamide was synthesized and studied. The impetus for this is the suggestion that in the presence of water, the formamido moiety could form a hydrate (*12*). Accordingly, hydration of the N-terminal formamido of polyamide could alter the planar sp^2 hybridized geometry of the carbonyl group to a more "tetrahedral-like" state. Such a change could cause the two stacked polyamide units to align in a staggered format, which would increase the level of interactions between the polyamides and DNA. By labeling the formamido carbon atom, we are able to investigate this idea using ^{13}C NMR techniques. The ^{13}C-labeled molecule **6** behaved identically to f-IPI **1** in all of the experiments described above. NMR analyses were performed with **6** using a decamer containing the staggered cognate sequence ACGCGT (CGCGnmr) as used in previous NMR studies of f-IPI (**1**) (*14*). The ^{1}H NMR spectrum of the 2:1 complex of polyamide **6** with CGCGnmr was identical to that reported for f-IPI (**1**) bound to the same decamer (data not shown). The ^{13}C NMR spectrum of the 2:1 complex of ^{13}C-f-IPI (**6**) and ACGCGT (CGCGnmr) gave only one signal at 162 ppm

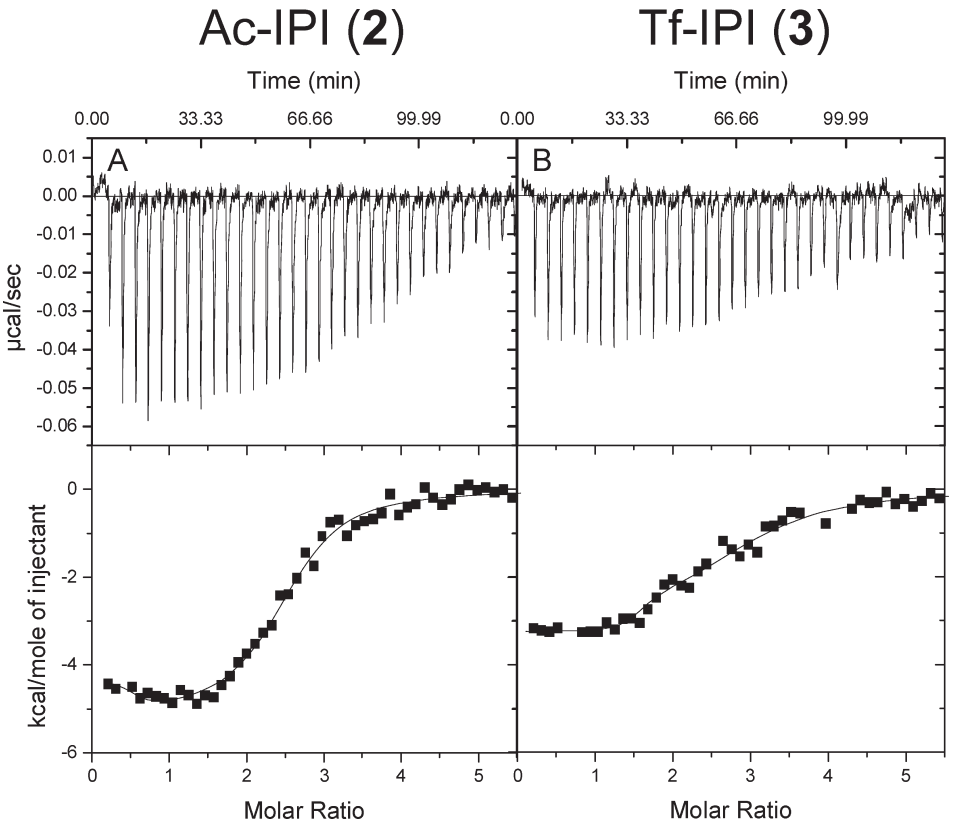

FIGURE 5: ITC thermograms (top) and integrated data (bottom) of (A) Ac-IPI (**2**) and (B) Tf-IPI (**3**) for binding to ACGCGT.

(external reference was $CDCl_3$ at 77 ppm). In comparison, the ^{13}C NMR signal of the ligand dissolved in the same phosphate buffer was recorded at 158 ppm (data not shown). These results provide evidence that binding of f-IPI (**1** or **6**) to ACGCGT is not likely to involve the formation of a hydrated formamido group, as that would have resulted in an upfield shift of the signal. The ^{13}C NMR signal for an acetal carbon is in the range of 90−100 ppm (*24*).

DNase I Footprinting. To further corroborate the sequence selectivity of compounds **1**−**8**, DNase I footprinting experiments on **1** and **3** were performed using a 130 bp 5′-^{32}P-radiolabeled DNA fragment containing the following sequences: 5′-ACGCGT-3′, 5′-ATGCAT-3′, 5′-AAATTT-3′, 5′-TAGCTT-3′, and 5′-ACTAGT-3′. The autoradiogram given in Figure 6 shows that a footprint appears at the 5′-ACGCGT-3′ cognate site from 0.05 μM for compound **1** and 5 μM for **3**. Secondary binding sites containing the sequences 5′-ATGCAT-3′ and 5′-TAGCTT-3′ were also observed at concentrations of ≥1 μM only with compound **1**.

DNase I footprinting experiments were performed with compounds **2** and **7** using a second DNA of a 130 bp 5′-^{32}P-radiolabeled DNA fragment containing the following sequences: 5′-ACGCGT-3′, 5′-ACCGGT-3′, 5′-AAATTT-3′, 5′-ACGTGT-3′, and 5′-AGCGCT-3′. Binding was observed at the cognate site (5′-ACGCGT-3′) for compounds **2** and **7** at 0.1 and 10 μM, respectively. From 10 μM, minor binding sites were also observed only for **2** at 5′-ACCGGT-3′, 5′-ACGTGT-3′, and 5′-AGCGCT-3′. In contrast, evidence of nonspecific binding was observed for **7** at doses above 10 μM. These results provide an indication that modification of the N-terminal acylamido can modestly improve sequence specificity, which affirm the results obtained from the aforementioned biophysical studies. However, as anticipated from earlier results (*10*), changes to the N-terminus significantly lowered binding affinity (Table 1).

Molecular Modeling Studies. Molecular visualization studies of the complexes of acyl-IPI with ACGCGT were conducted using the Tripos SYBYL modeling and visualization package. On the basis of the published structure of staggered polyamide binding, e.g., f-IPI (**1**) (*14*), the polyamide was docked as a side-by-side stacked dimer in the minor groove. A short molecular mechanics minimization (Tripos force field) was used again to optimze the structure. The N-terminus of the polyamide was then modified to each acyl group as described in the paper. After another short molecular mechanics optimization run, the interatomic distances were evaluated by standard methods in SYBYL.

Modeling studies clearly show that f-IPI fits nicely into the minor groove of the cognate ACGCGT sequence and can hydrogen bond (NH to base acceptors) very effectively with electron-rich atoms on the floor of the minor groove. The N-terminal "H" of "f" fits into the groove and approaches the floor of the groove without steric clash while providing favorable stacking geometry and energetics with the opposite molecule of the stacked dimer. With a CH_3 group in place of the H, some steric clash with the bases at the floor of the groove occurs and requires conformational rearrangement. Although rearrangement can occur, it costs energy and can lead to additional clash within the stacked dimer. A CF_3 group causes similar problems. The observed effects with both compounds are basically due to the polyamide being slightly too curved to match the minor groove shape as the trimer system is extended. This also causes some unfavorable interactions with a four-ring system, and the expected binding enhancement is not seen on extending the trimer f-IPI polyamide.

With the N-amino and non-f compounds, some of the favorable stacking energetics and van der Waals interactions with the groove walls and opposite molecule in the dimer are lost.

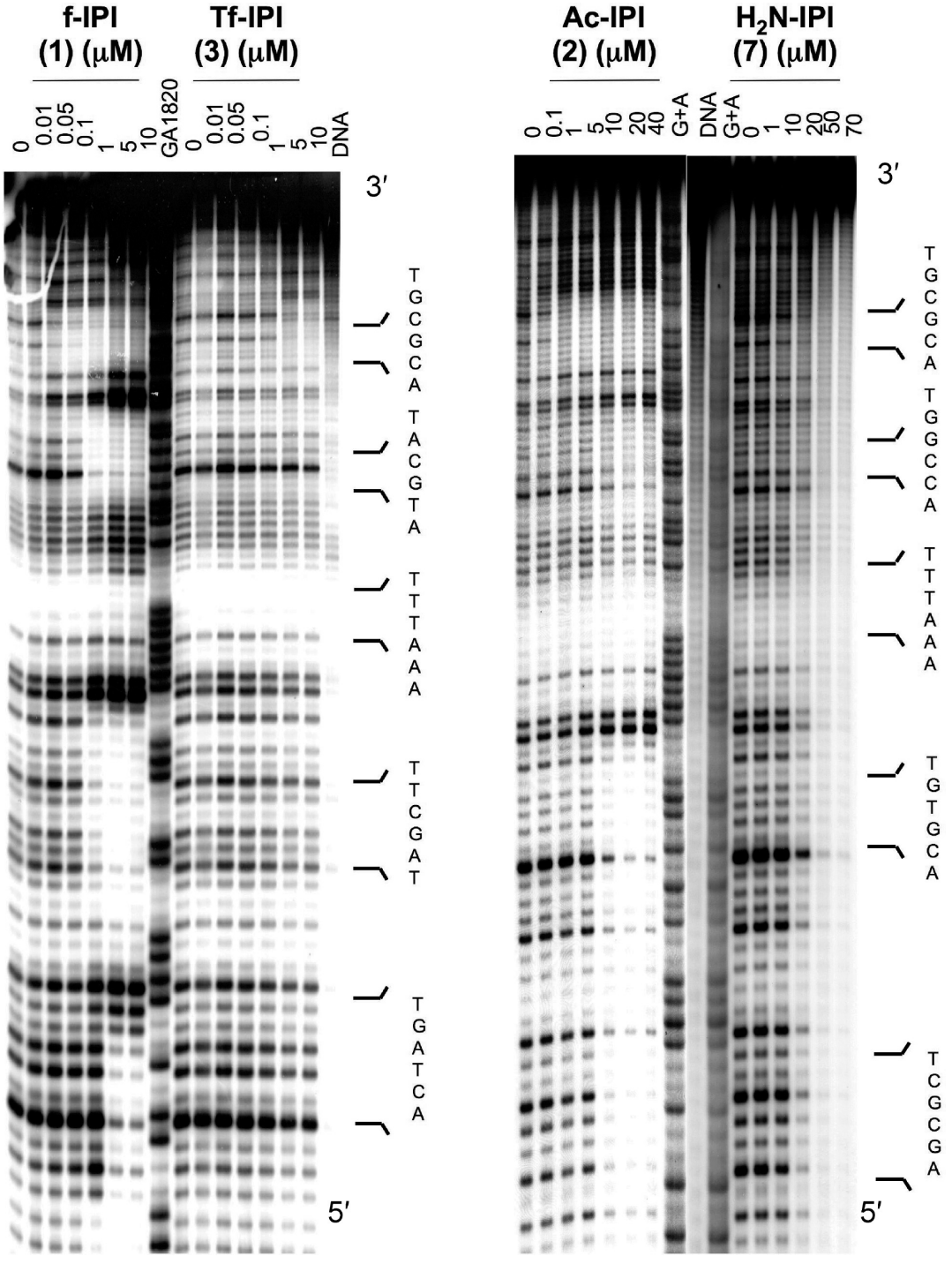

FIGURE 6: DNase I footprinting of compounds **1**−**3** and **7** using two different 130 bp 5′-^{32}P-radiolabeled DNA fragments showing the sites 5′-ACGCGT-3′, 5′-ATGCAT-3′, 5′-AAATTT-3′, 5′-TAGCTT-3′, and 5′-ACTAGT-3′ (left) or 5′-ACGCGT-3′, 5′-ACCGGT-3′, 5′-AAATTT-3′, 5′-ACGTGT-3′, and 5′-AGCGCT-3′ (right). DNA is the undigested control, and G + A is the sequencing lane.

CONCLUSIONS

A number of important conclusions can be deduced from these results. (1) Having an acylamido group at the N-termini of polyamides is crucial for improving DNA binding affinity. Consistent with the formamido group, the *N*-acylamido groups also promoted the polyamides to bind ACGCGT through the stacked and staggered motif. (2) Increasing steric bulk at the N-terminus (**1**−**4**) reduces binding affinity. (3) Adding polar atoms, such as fluorine atoms to Tf (**3**) and a *N*-methylamino group to Mu (**4**), to the N-terminal acylamido group has little effect on binding affinity. (4) Replacing the formamido group can lead to an enhancement in sequence preference (**1**−**5**), but at the expense of binding affinity. Even though these findings are important and they add to our understanding of how polyamide analogues of distamycin bind DNA, the fundamental questions of why the formamido group has such a dramatic effect in enhancing the binding constant and why *N*-acylamido compounds prefer to stack in a staggered fashion remain to be answered.

REFERENCES

1. Arcamone, F., Penco, S., Orezzi, P., Nicolella, V., and Pirelli, A. (1964) Synthesis of Distamycin A. *Nature 203*, 1064–1065.

2. Dervan, P. B. (2001) Molecular recognition of DNA by Small Molecules. *Bioorg. Med. Chem. 9*, 2215–2235.
3. Pelton, J. G., and Wemmer, D. E. (1989) Structural characterization of a 2:1 distamycin A:d(CGCAAATTGGC) complex by two-dimensional NMR. *Proc. Natl. Acad. Sci. U.S.A. 86*, 5723–5727.
4. Dwyer, T. J., Geierstanger, B. H., Bathini, Y., Lown, J. W., and Wemmer, D. E. (1992) Design and binding of a distamycin A analog to d(CGCAAGTTGGC) d(GCCAACTTGCG): Synthesis, NMR studies, and implications for the design of sequence-specific minor groove binding oligopeptides. *J. Am. Chem. Soc. 114*, 5911–5919.
5. Wade, W. S., Mrksich, M., and Dervan, P. B. (1992) Design of peptides that bind in the minor groove of DNA at 5′-(A,T)G(A,T)C(A,T)-3′ sequences by a dimeric side-by-side motif. *J. Am. Chem. Soc. 114*, 8783–8794.
6. Mrksich, M., Wade, W. S., Dwyer, T. J., and Geierstanger, B. (1992) Antiparallel side-by-side dimeric motif for sequence-specific recognition in the minor groove of DNA by the designed peptide 1-methylimidazole-2-carboxamide netropsin. *Proc. Natl. Acad. Sci. U.S.A. 89*, 7586–7590.
7. Kielkopf, C. L., Baird, E. E., Dervan, P. B., and Rees, D. C. (1998) Structural basis for G·C recognition in the DNA minor groove. *Nat. Struct. Biol. 5*, 104–109.
8. Buchmueller, K. L., Staples, A. M., Howard, C. M., Horick, S. M., Uthe, P. B., Le, N. M., Cox, K. K., Nguyen, B., Pacheco, K. A. O., Wilson, W. D., and Lee, M. (2005) Extending the language of DNA molecular recognition by polyamides: Unexpected influence of imidazole and pyrrole arrangement on binding affinity and specificity. *J. Am. Chem. Soc. 127*, 742–750.
9. Swalley, S., Baird, E. E., and Dervan, P. B. (1997) Discrimination of 5′-GGGG-3′, 5′-GCGC-3′, and 5′-GGCC-3′ sequences in the minor groove of DNA by eight-ring hairpin polyamides. *J. Am. Chem. Soc. 119*, 6953–6961.
10. Lacy, E., Minh Le, N., Price, C., Lee, M., and Wilson, W. D. (2002) Influence of a terminal formamido group on the sequence recognition of DNA by polyamides. *J. Am. Chem. Soc. 124*, 2153–2163.
11. White, S., Barid, E. E., and Dervan, P. B. (1997) Orientation preferences of pyrrole-imidazole polyamides in the minor groove of DNA. *J. Am. Chem. Soc. 119*, 8756–8765.
12. (a) Marchese, F. T., Mehrotra, P. K., and Beveridge, D. L. (1984) Monte Carlo study of the aqueous hydration of formamide at 25 °C. *J. Phys. Chem. 88*, 5692–5702. (b) Wolfenden, R. (1976) Free energies of hydration and hydrolysis of gaseous acetamide. *J. Am. Chem. Soc. 98*, 1987–1988.
13. Brown, T., Mackay, H., Turlington, M., Sutterfield, A., Smith, T., Sielaff, A., Westrate, L., Bruce, C., Kluza, J., O'Hare, C., Nguyen, B., Wilson, W. D., Hartley, J. A., and Lee, M. (2008) Modifying the *N*-terminus of polyamides: PyImPyIm has improved sequence specificity over f-ImPyIm. *Bioorg. Med. Chem. 16*, 5266–5276.
14. Buchmueller, K. L., Bailey, S. L., Matthews, D. A., Taherbhai, Z. T., Register, J. K., Davis, Z. S., Bruce, C. D., O'Hare, C., Hartley, J. A., and Lee, M. (2006) Physical and structural basis for the strong interactions of the -ImPY- central pairing motif in the polyamide f-ImPyIm. *Biochemistry 45*, 13551–13565.
15. Brown, T., Taherbhai, Z., Sexton, J., Sutterfield, A., Turlington, M., Jones, J., Stallings, L., Stewart, M., Buchmueller, K., Mackay, H., O'Hare, C., Kluza, J., Nguyen, B., Wilson, D., Lee, M., and Hartley, J. A. (2007) Synthesis and biophysical evaluation of minor-groove binding C-terminus modified pyrrole and imidazole triamide analogs of distamycin. *Bioorg. Med. Chem. 15*, 474–483.
16. Flores, L. V., Staples, A. M., Mackay, H., Howard, C. M., Uthe, P. B., Sexton, J. S., Buchmueller, K. L., Wilson, W. D., O'Hare, C., Kluza, J., Hochhauser, D., Hartley, J. A., and Lee, M. (2006) Synthesis and evaluation of an intercaltor-polyamide hairpin designed to target the inverted CCAAT box 2 in the topoisomerase IIα promoter. *ChemBioChem 7*, 1722–1729.
17. Sielaff, A., Mackay, H., Brown, T., and Lee, M. (2008) 2-Aminopurine/cytosine base pair containing oligonucleotides: Fluorescence spectroscopy studies on DNA-polyamide binding. *Biochem. Biophys. Res. Commun. 369*, 630–634.
18. Indyk, L., and Fisher, H. F. (1998) Theoretical aspects of isothermal titration calorimetry. *Methods Enzymol. 295*, 350–364.
19. (a) Nguyen, B., Tanious, F. A., and Wilson, W. D. (2007) Biosensor-surface plasmon resonance: Quantitative analysis of small molecule-nucleic acid interactions. *Methods 42*, 150–161. (b) Wilson, W. D. (2002) Analyzing Biomolecular Interactions. *Science 295*, 2103–2105. (c) Lacy, E. R., Le, N. M., Price, C. A., Lee, M., and Wilson, W. D. (2002) Influence of a terminal formamido group on the sequence recognition of DNA by polyamides. *J. Am. Chem. Soc. 124*, 2153–2163.
20. Mackay, H., Brown, T., Uthe, P. B., Westrate, L., Sielaff, A., Jones, J., Lajiness, J. P., Kluza, J., O'Hare, C., Nguyen, B., Davis, Z., Bruce, C., Wilson, W. D., Hartley, J. A., and Lee, M. (2008) Sequence specific and high affinity recognition of 5′-ACGCGT-3′ by rationally designed pyrrole-imidazole H-pin polyamides: Thermodynamic and structural studies. *Bioorg. Med. Chem. 16*, 9145–9153.
21. (a) Lyng, R., Rodger, A., and Norden, B. (1991) The CD of ligand-DNA systems. I. Poly(dG-dC) B-DNA. *Biopolymers 31*, 1709–1720. (b) Lyng, R., Rodger, A., and Norden, B. (1992) The CD of ligand-DNA systems. 2. Poly(dA-dT) B-DNA. *Biopolymers 32*, 1201–1214.
22. (a) Yang, X. L., Hubbard, R. B.IV, Lee, M., Tao, Z. F., Sugiyama, H., and Wang, A. H. (1999) Imidazole-imidazole pair as a minor groove recognition motif for T:G mismatched base pairs. *Nucleic Acids Res. 27*, 4183–4190. (b) Parks, M. E., Baird, E. E., and Dervan, P. B. (1996) Optimization of the Hairpin Polyamide Design for Recognition of the Minor Groove of DNA. *J. Am. Chem. Soc. 118*, 6147–6152. (c) Hawkins, C. A., Peláez, R., Dominey, R. N., Baird, E. E., White, S., Dervan, P. B., and Wemmer, D. E. (2000) Controlling Binding Orientation in Hairpin Polyamide DNA Complexes. *J. Am. Chem. Soc. 122*, 5235–5243.
23. http://www.molinspiration.com/services/volume.html (accessed January 1, 2009).
24. Silverstein, R. M., and Webster, F. X. (1997) Spectrometric Identification of Organic Compounds , 6th ed., John Wiley & Sons, New York.